High-Rate Space-Time Coded Large MIMO Systems: Low-Complexity Detection and Performance

Saif K. Mohammed, A. Chockalingam, B. Sundar Rajan
Department of ECE, Indian Institute of Science, Bangalore 560012, INDIA

***Abstract*— Large MIMO systems with tens of antennas in each communication terminal using full-rate non-orthogonal space-time block codes (STBC) from Cyclic Division Algebras (CDA) can achieve the benefits of both transmit diversity as well as high spectral efficiencies. Maximum-likelihood (ML) or near-ML decoding of these large-sized STBCs at low complexities, however, has been a challenge. In this paper, we establish that near-ML decoding of these large STBCs is possible at practically affordable low complexities. We show that the likelihood ascent search (LAS) detector, reported earlier by us for V-BLAST, is able to achieve near-ML uncoded BER performance in decoding a 32×32 STBC from CDA, which employs 32 transmit antennas and sends $32^2 = 1024$ complex data symbols in 32 time slots in one STBC matrix (i.e., 32 data symbols sent per channel use). In terms of coded BER, with a 16×16 STBC, rate-3/4 turbo code and 4-QAM (i.e., 24 bps/Hz), the LAS detector performs close to within just about 4 dB from the theoretical MIMO capacity. Our results further show that, with LAS detection, information lossless (ILL) STBCs perform almost as good as full-diversity ILL (FD-ILL) STBCs. Such low-complexity detectors can potentially enable implementation of high spectral efficiency large MIMO systems that could be considered in wireless standards.**

Keywords *– Large MIMO systems, full-rate non-orthogonal STBCs, low-complexity detection, high spectral efficiency.*

I. INTRODUCTION

Current wireless standards (e.g., IEEE 802.11n, 802.16e) have adopted MIMO techniques [1]-[3] to achieve transmit diversity (using space-time coding) and high data rates (using spatial multiplexing). They, however, harness only a limited potential of MIMO benefits since they use only a small number of antennas (e.g., 2 to 4 antennas in 802.11n and 802.16e). Significant benefits can be realized if large number of antennas are used; e.g., large MIMO systems with *several tens of antennas* in communication terminals can enable multi-giga bit rate transmissions at high spectral efficiencies of the order of *several tens of bps/Hz*[1]. Key challenges in realizing such large MIMO systems include low-complexity detection, channel estimation, RF/IF technologies, and placement of large number of antennas in communication terminals[2]. Our focus in this paper is on low-complexity detection in large space-time coded MIMO systems.

Spatial multiplexing (V-BLAST) with large number of antennas can offer high spectral efficiencies, but it does not provide transmit diversity [2]. On the other hand, well known orthogonal space-time block codes (STBC) have the advantages of full transmit diversity and low decoding complexity, but suffer from rate loss for increasing number of transmit antennas [3],[4],[5]. In this regard, we point out that *full-rate non-orthogonal STBCs from Cyclic Division Algebras (CDA)* [6] are attractive to achieve high spectral efficiencies in addition to achieving full transmit diversity, using large number of transmit antennas. However, while maximum-likelihood (ML) decoding of orthogonal STBCs can be achieved in just linear complexity, ML or near-ML decoding of non-orthogonal STBCs from CDA gets prohibitively complex for large number of transmit antennas. Consequently, a key challenge in realizing the benefits of these full-rate non-orthogonal STBCs in practice is that of achieving near-ML performance for large number of transmit antennas at low complexities. Our main contribution in this paper is that we establish that near-ML decoding of large non-orthogonal STBCs from CDA is possible at practically affordable low complexities.

Sphere decoding and several of its low-complexity variants are known in the literature [7]-[9]. These detectors, however, are prohibitively complex for large number of antennas. Recent approaches to low-complexity multiuser/MIMO detection involve application of techniques from belief propagation [10], Markov Chain Monte-Carlo methods [11], neural networks [12],[13],[14], etc. In particular, in [13],[14], we presented a powerful Hopfield neural network based MIMO detection algorithm, termed as likelihood ascent search (LAS) algorithm, and demonstrated its near-ML performance at low complexities in large MIMO systems with tens to hundreds of antennas. A multistage version of the LAS algorithm, termed as M-LAS algorithm, and a method to obtain soft outputs from the LAS algorithm are presented in [15].

In this paper, we adopt the LAS algorithm to decode large STBCs from CDA and report interesting results. Assuming i.i.d. Rayleigh fading and perfect channel knowledge at the receiver, we show that the LAS algorithm is able to decode large non-orthogonal STBCs (e.g., 16×16 and 32×32 STBCs from CDA) and achieve near SISO AWGN uncoded BER performance as well as near-capacity (within 4 dB from theoretical MIMO capacity) coded BER performance. We note that decoding and BER performance of large non-orthogonal STBCs like the 32×32 STBC from CDA have not been reported so far. The low-complexity attribute of the LAS detector further allows us to study the performance difference between STBCs operated at high spectral efficiencies, in relation to their full-diversity (FD) and information losslessness (ILL) features. Our results show that the performance of 'ILL-only' STBCs is almost the same as that of 'FD and ILL' (FD-ILL) STBCs, suggesting that, in such cases, the simplicity of ILL-only STBCs can be taken advantage of without incurring much performance loss compared to FD-ILL STBCs. LAS detection performance for $N_r < N_t$ is also presented.

[1]Spectral efficiencies achieved in current MIMO wireless standards are only about 10 bps/Hz or less.

[2]We note that there can be several large MIMO applications where antenna placement need not be a major issue. An example of such a scenario is high-speed backbone connectivity between base stations using large MIMO links, where large number of antennas can be placed at the base stations. Also, tens of antennas can be placed in moderately sized terminals (e.g., laptops, set top boxes) that can enable interesting spectrally efficient, high data rate applications like wireless IPTV distribution.

978-1-4244-2324-8/08/$25.00 © 2008 IEEE.

II. STBC MIMO System Model

Consider a space-time block coded MIMO system with multiple transmit and receive antennas. An (n, p, k) STBC is represented by a matrix $\mathbf{X}_c \in \mathbb{C}^{n\times p}$, where n and p denote the number of transmit antennas and number of time slots, respectively, and k denotes the number of complex data symbols sent in one STBC matrix. The (i, j)th entry in $\mathbf{X}_c$ represents the complex number transmitted from the ith transmit antenna in the jth time slot. The rate of an STBC, r, is $r \triangleq \frac{k}{p}$. Let N_r and $N_t = n$ denote the number of receive and transmit antennas, respectively. We assume quasi-static fading, where the channel gains are assumed to remain constant over one STBC block and vary (i.i.d) from one STBC block to the other. Let $\mathbf{H}_c \in \mathbb{C}^{N_r\times N_t}$ denote the channel gain matrix, where the (i, j)th entry in $\mathbf{H}_c$ is the complex channel gain from the jth transmit antenna to the ith receive antenna. Assuming rich scattering, we model the entries of $\mathbf{H}_c$ as i.i.d $\mathcal{CN}(0, 1)$. The received space-time signal matrix, $\mathbf{Y}_c \in \mathbb{C}^{N_r\times p}$, can be written as

$$\mathbf{Y}_c = \mathbf{H}_c\mathbf{X}_c + \mathbf{N}_c, \tag{1}$$

where $\mathbf{N}_c \in \mathbb{C}^{N_r\times p}$ is the noise matrix at the receiver and its entries are modeled as i.i.d $\mathcal{CN}\big(0, \sigma^2 = \frac{N_t E_s}{\gamma}\big)$, where E_s is the average energy of the transmitted symbols, and γ is the average received SNR per receive antenna [3], and the (i, j)th entry in $\mathbf{Y}_c$ is the received signal at the ith receive antenna in the jth time-slot. In a linear dispersion (LD) STBC [3], $\mathbf{X}_c$ can be decomposed into a linear combination of weight matrices corresponding to each data symbol and its conjugate as

$$\mathbf{X}_c = \sum_{i=1}^{k} x_c^{(i)}\mathbf{A}_c^{(i)} + (x_c^{(i)})^*\mathbf{E}_c^{(i)}, \tag{2}$$

where $x_c^{(i)}$ is the ith complex data symbol, and $\mathbf{A}_c^{(i)}, \mathbf{E}_c^{(i)} \in \mathbb{C}^{N_t\times p}$ are its corresponding weight matrices. The LAS detection algorithm we presented in [13],[14] can decode general LD STBCs of the form in (2). For the purpose of simplicity in exposition, here we consider a subclass of LD STBCs, where $\mathbf{X}_c$ can be written in the form

$$\mathbf{X}_c = \sum_{i=1}^{k} x_c^{(i)}\mathbf{A}_c^{(i)}. \tag{3}$$

Applying the $vec\,(.)$ operation on $\mathbf{Y}_c$ and using (2), we have

$$vec\,(\mathbf{Y}_c) = \sum_{i=1}^{k} x_c^{(i)} vec\,(\mathbf{H}_c\mathbf{A}_c^{(i)}) + vec\,(\mathbf{N}_c). \tag{4}$$

If $\mathbf{U}$,$\mathbf{V}$,$\mathbf{W}$,$\mathbf{D}$ are matrices such that $\mathbf{D} = \mathbf{UWV}$, then it is true that $vec\,(\mathbf{D}) = (\mathbf{V}^T \otimes \mathbf{U})\, vec\,(\mathbf{W})$, where $\otimes$ denotes the tensor product of matrices. Using this, we can write (4) as

$$vec\,(\mathbf{Y}_c) = \sum_{i=1}^{k} x_c^{(i)}(\mathbf{I} \otimes \mathbf{H}_c)\, vec\,(\mathbf{A}_c^{(i)}) + vec\,(\mathbf{N}_c), \tag{5}$$

where $\mathbf{I}$ is the $p \times p$ identity matrix. Further, define $\mathbf{y}_c \triangleq vec\,(\mathbf{Y}_c)$, $\widehat{\mathbf{H}}_c \triangleq (\mathbf{I} \otimes \mathbf{H}_c)$, $\mathbf{a}_c^{(i)} \triangleq vec\,(\mathbf{A}_c^{(i)})$, and $\mathbf{n}_c \triangleq vec\,(\mathbf{N}_c)$. From these definitions, it is clear that $\mathbf{y}_c \in \mathbb{C}^{N_r p\times 1}$, $\widehat{\mathbf{H}}_c \in \mathbb{C}^{N_r p\times N_t p}$, $\mathbf{a}_c^{(i)} \in \mathbb{C}^{N_t p\times 1}$, and $\mathbf{n}_c \in \mathbb{C}^{N_r p\times 1}$. Let us also define a matrix $\widetilde{\mathbf{H}}_c \in \mathbb{C}^{N_r p\times k}$, whose ith column is $\widehat{\mathbf{H}}_c\,\mathbf{a}_c^{(i)}$, $i = 1, \cdots, k$. Let $\mathbf{x}_c \in \mathbb{C}^{k\times 1}$, whose ith entry is the data symbol $x_c^{(i)}$. With these definitions, we can write (5) as

$$\mathbf{y}_c \;=\; \sum_{i=1}^{k} x_c^{(i)}\,(\widehat{\mathbf{H}}_c\,\mathbf{a}_c^{(i)}) + \mathbf{n}_c \;=\; \widetilde{\mathbf{H}}_c\mathbf{x}_c + \mathbf{n}_c. \tag{6}$$

Each element of $\mathbf{x}_c$ is an M-PAM or M-QAM symbol. M-PAM symbols take discrete values from $\{A_m, m = 1, \cdots, M\}$, where $A_m = (2m-1-M)$, and M-QAM is nothing but two PAMs in quadrature. Let $\mathbf{y}_c$, $\widetilde{\mathbf{H}}_c$, $\mathbf{x}_c$, and $\mathbf{n}_c$ be decomposed into real and imaginary parts as follows:

$$\begin{aligned} \mathbf{y}_c &= \mathbf{y}_I + j\mathbf{y}_Q, \quad \mathbf{x}_c = \mathbf{x}_I + j\mathbf{x}_Q, \\ \mathbf{n}_c &= \mathbf{n}_I + j\mathbf{n}_Q, \quad \widetilde{\mathbf{H}}_c = \mathbf{H}_I + j\mathbf{H}_Q. \end{aligned} \tag{7}$$

Further, we define $\mathbf{H}_r \in \mathbb{R}^{2N_r p\times 2k}$, $\mathbf{y}_r \in \mathbb{R}^{2N_r p\times 1}$, $\mathbf{x}_r \in \mathbb{R}^{2k\times 1}$, and $\mathbf{n}_r \in \mathbb{R}^{2N_r p\times 1}$ as

$$\mathbf{H}_r = \begin{pmatrix} \mathbf{H}_I & -\mathbf{H}_Q \\ \mathbf{H}_Q & \mathbf{H}_I \end{pmatrix}, \quad \mathbf{y}_r = [\mathbf{y}_I^T \;\; \mathbf{y}_Q^T]^T, \tag{8}$$

$$\mathbf{x}_r = [\mathbf{x}_I^T \;\; \mathbf{x}_Q^T]^T, \quad \mathbf{n}_r = [\mathbf{n}_I^T \;\; \mathbf{n}_Q^T]^T. \tag{9}$$

Now, (6) can be written as

$$\mathbf{y}_r = \mathbf{H}_r\mathbf{x}_r + \mathbf{n}_r. \tag{10}$$

Henceforth, we work with the real-valued system in (10). For notational simplicity, we drop subscripts r in (10) and write

$$\mathbf{y} = \mathbf{H}\mathbf{x} + \mathbf{n}, \tag{11}$$

where $\mathbf{H} = \mathbf{H}_r \in \mathbb{R}^{2N_r p\times 2k}$, $\mathbf{y} = \mathbf{y}_r \in \mathbb{R}^{2N_r p\times 1}$, $\mathbf{x} = \mathbf{x}_r \in \mathbb{R}^{2k\times 1}$, and $\mathbf{n} = \mathbf{n}_r \in \mathbb{R}^{2N_r p\times 1}$. We assume that the channel coefficients are known at the receiver but not at the transmitter. Let $\mathbb{A}_i$ denote the M-PAM signal set from which x_i (ith entry of $\mathbf{x}$) takes values, $i = 1, \cdots, 2k$. Now, define a $2k$-dimensional signal space $\mathbb{S}$ to be the Cartesian product of $\mathbb{A}_1$ to $\mathbb{A}_{2k}$. The ML solution is then given by

$$\mathbf{d}_{ML} \;=\; \underset{\mathbf{d}\,\in\,\mathbb{S}}{\arg\min}\; \mathbf{d}^T\mathbf{H}^T\mathbf{H}\mathbf{d} - 2\mathbf{y}^T\mathbf{H}\mathbf{d}, \tag{12}$$

whose complexity is exponential in k.

A. Full-rate Non-orthogonal STBCs from CDA

We focus on the detection of square (i.e., $n = p = N_t$), full-rate (i.e., $k = pn = N_t^2$), circulant (where the weight matrices $\mathbf{A}_c^{(i)}$'s are permutation type), non-orthogonal STBCs from CDA [6], whose construction for arbitrary number of transmit antennas n is given by the matrix in (12.a) given at the bottom of the next page. In (12.a), $\omega_n = e^{\frac{\mathbf{j}2\pi}{n}}$, $\mathbf{j} = \sqrt{-1}$, and $x_{u,v}$, $0 \le u, v \le n-1$ are the data symbols from a QAM alphabet. When $\delta = e^{\sqrt{5}\mathbf{j}}$ and $t = e^{\mathbf{j}}$, the STBC in (12.a) achieves full transmit diversity (under ML decoding) as well as information-losslessness [6]. When $\delta = t = 1$, the code ceases to be of full-diversity (FD), but continues to be information-lossless (ILL) [16]. High spectral efficiencies with large n can be achieved using this code construction. For example, with $n = 32$ transmit antennas, the 32×32 STBC from (12.a) with 16-QAM and rate-3/4 turbo code achieves a spectral efficiency of 96 bps/Hz. This high spectral efficiency is achieved along with the full diversity of order nN_r. However, since these STBCs are non-orthogonal, ML detection gets increasingly impractical for large n. Consequently, a key challenge in realizing the benefits of these large STBCs in practice is that of achieving near-ML performance for large n at low decoding complexities. Our simulation results in Sec. IV show that the LAS detection algorithm, reported by us in [13],[14] for V-BLAST and summarized in the next section, essentially meets this challenge.

III. LAS Algorithm for Large MIMO Detection

The LAS algorithm starts with an initial vector $\mathbf{d}^{(0)}$, given by $\mathbf{d}^{(0)} = \mathbf{B}\mathbf{y}$, where $\mathbf{B}$ is the initial solution filter, which can be a matched filter (MF) or zero-forcing (ZF) filter or MMSE filter. The index m in $\mathbf{d}^{(m)}$ denotes the iteration number in a given search stage. The ML cost function after the kth iteration in a given search stage is given by

$$C^{(k)} \;=\; \mathbf{d}^{(k)^T}\mathbf{H}^T\mathbf{H}\mathbf{d}^{(k)} - 2\mathbf{y}^T\mathbf{H}\mathbf{d}^{(k)}. \qquad (13)$$

The $\mathbf{d}$ vector is updated from kth to $(k+1)$th iteration by updating one symbol, say, the pth symbol, as

$$\mathbf{d}^{(k+1)} \;=\; \mathbf{d}^{(k)} + \lambda_p^{(k)}\mathbf{e}_p, \qquad (14)$$

where $\mathbf{e}_p$ denotes the unit vector with its pth entry only as one, and all other entries as zero. Since $\mathbf{d}^{(k)}$ and $\mathbf{d}^{(k+1)}$ should belong to $\mathbb{S}$, $\lambda_p^{(k)}$ can take only certain integer values. For example, for 16-QAM, $\mathbb{A}_p = \{-3,-1,1,3\}$, and $\lambda_p^{(k)}$ can take values only from $\{-6,-4,-2,0,2,4,6\}$. Using (13) and (14), and defining a matrix $\mathbf{G}$ as

$$\mathbf{G} \;\triangleq\; \mathbf{H}^T\mathbf{H}, \qquad (15)$$

we can write the cost difference $C^{(k+1)} - C^{(k)}$ as

$$\mathcal{F}(l_p^{(k)}) \;\triangleq\; C^{(k+1)} - C^{(k)} \;=\; {l_p^{(k)}}^2 a_p - 2l_p^{(k)}|z_p^{(k)}|, \qquad (16)$$

where $z_p^{(k)}$ is the pth entry of the $\mathbf{z}^{(k)}$ vector given by $\mathbf{z}^{(k)} = \mathbf{H}^T(\mathbf{y} - \mathbf{H}\mathbf{d}^{(k)})$, $a_p \triangleq (\mathbf{G})_{p,p}$ is the (p,p)th entry of the $\mathbf{G}$ matrix, and $l_p^{(k)} = |\lambda_p^{(k)}|$. The value of $l_p^{(k)}$ which gives the largest descent in the cost function from the kth to the $(k+1)$th iteration (when symbol p is updated) is obtained as

$$l_{p,opt}^{(k)} \;=\; 2\left\lfloor \frac{|z_p^{(k)}|}{2a_p} \right\rceil, \qquad (17)$$

where $\lfloor . \rceil$ denotes the rounding operation. If $d_p^{(k)}$ were updated using $l_{p,opt}^{(k)}$, it is possible that the updated value does not belong to $\mathbb{A}_p$. To avoid this, we adjust $l_{p,opt}^{(k)}$ so that the updated value of $d_p^{(k)}$ belongs to $\mathbb{A}_p$. Let

$$s \;=\; \underset{p}{\arg\min}\; \mathcal{F}(l_{p,opt}^{(k)}). \qquad (18)$$

If $\mathcal{F}(l_{s,opt}^{(k)}) < 0$, the update for the $(k+1)$th iteration is

$$\mathbf{d}^{(k+1)} \;=\; \mathbf{d}^{(k)} + l_{s,opt}^{(k)}\mathrm{sgn}(z_s^{(k)})\mathbf{e}_s \qquad (19)$$

$$\mathbf{z}^{(k+1)} \;=\; \mathbf{z}^{(k)} - l_{s,opt}^{(k)}\mathrm{sgn}(z_s^{(k)})\mathbf{g}_s, \qquad (20)$$

where $\mathbf{g}_s$ is the sth column of $\mathbf{G}$. If $\mathcal{F}(l_{s,opt}^{(k)}) \geq 0$, then the search terminates. In an uncoded system, $\mathbf{d}^{(k)}$ is declared as the detected data vector. In coded systems, however, soft inputs to the decoder are preferred.

A. Generation of Soft Outputs

Soft values at the LAS algorithm output can be generated for the individual bits that constitute the M-QAM symbols as described in [15]. These soft outputs can then be fed as inputs to the decoder in coded systems. Let $\mathbf{d} = [\widehat{x}_1, \widehat{x}_2, \cdots, \widehat{x}_{2N_t^2}]$, $\widehat{x}_i \in \mathbb{A}_i$ denote the detected output vector from the LAS algorithm. Let $\widehat{x}_i$ map to the bit vector $\mathbf{b}_i = [b_{i,1}, b_{i,2}, \cdots, b_{i,K_i}]^T$, where $K_i = \log_2|\mathbb{A}_i|$, and $b_{i,j} \in \{+1,-1\}$, $i = 1,2,\cdots,2N_t^2$ and $j = 1,2,\cdots,K_i$. Let $\tilde{b}_{i,j} \in \mathbb{R}$ denote the soft value for the jth bit of the ith symbol. Given $\mathbf{d}$, we need to find $\tilde{b}_{i,j}$, $\forall\,(i,j)$.

Define vectors $\mathbf{b}_i^{j+}$ and $\mathbf{b}_i^{j-}$ to be the $\mathbf{b}_i$ vector with its jth entry forced to +1 and -1, respectively. Let $\mathbf{b}_i^{j+}$ and $\mathbf{b}_i^{j-}$ demap to x_i^{j+} and x_i^{j-}, respectively, where $x_i^{j+}, x_i^{j-} \in \mathbb{A}_i$. Also, define vectors $\mathbf{d}_i^{j+}$ and $\mathbf{d}_i^{j-}$ to be the $\mathbf{d}$ vector with its ith entry forced to x_i^{j+} and x_i^{j-}, respectively. Using the above definitions, we obtain the soft output value for the jth bit of the ith symbol as

$$\tilde{b}_{i,j} \;=\; \frac{\|\mathbf{y} - \mathbf{H}\mathbf{d}_i^{j-}\|^2 - \|\mathbf{y} - \mathbf{H}\mathbf{d}_i^{j+}\|^2}{\|\mathbf{h}_i\|^2}. \qquad (21)$$

The RHS in the above can be efficiently computed in terms of $\mathbf{z}$ and $\mathbf{G}$ [15].

B. Computational Complexity of LAS Detection of STBCs

The complexity of the LAS algorithm comprises of three components, namely, i) computation of the initial vector $\mathbf{d}^{(0)}$, ii) computation of $\mathbf{H}^T\mathbf{H}$, and iii) the search operation. Figure 1 shows the per-symbol complexity plots (obtained through simulations) as a function of $N_t = N_r$ for 4-QAM at an SNR of 6 dB using MMSE initial vector. Two good properties of the STBCs from CDA are instrumental in achieving low orders of complexity for the computation of $\mathbf{d}^{(0)}$ and $\mathbf{H}^T\mathbf{H}$. They are: i) the weight matrices $\mathbf{A}_c^{(i)}$'s are *permutation type*, and ii) the $N_t^2 \times N_t^2$ matrix formed with $N_t^2 \times 1$-sized $\mathbf{a}_c^{(i)}$ vectors as columns is a *scaled unitary matrix*. These properties allow the computation of MMSE/ZF initial solution in $O(N_t^4)$ complexity, i.e., in $O(N_t^2)$ per-symbol complexity since there are N_t^2 symbols in a STBC matrix. Likewise, the computation of $\mathbf{H}^T\mathbf{H}$ can be done in $O(N_t^3)$ per-symbol complexity. The average per-symbol complexity of the search operation is of order $O(N_t^2)$. This can be observed from Fig. 1, where it can be seen that the per-symbol complexity in the initial vector computation plus the search operation is $O(N_t^2)$; this complexity plot runs parallel to the $c_1 N_t^2$ line. With the computation of $\mathbf{H}^T\mathbf{H}$ included, the complexity order is more than N_t^2. From the slopes of the plots in Fig. 1, we find that the overall per-symbol complexities for $N_t = 16$ and 32 are proportional to $N_t^{2.5}$ and $N_t^{2.7}$, respectively.

$$\begin{bmatrix}
\sum_{i=0}^{n-1} x_{0,i}\, t^i & \delta\sum_{i=0}^{n-1} x_{n-1,i}\, \omega_n^i\, t^i & \delta\sum_{i=0}^{n-1} x_{n-2,i}\, \omega_n^{2i}\, t^i & \cdots & \delta\sum_{i=0}^{n-1} x_{1,i}\, \omega_n^{(n-1)i}\, t^i \\
\sum_{i=0}^{n-1} x_{1,i}\, t^i & \sum_{i=0}^{n-1} x_{0,i}\, \omega_n^i\, t^i & \delta\sum_{i=0}^{n-1} x_{n-1,i}\, \omega_n^{2i}\, t^i & \cdots & \delta\sum_{i=0}^{n-1} x_{2,i}\, \omega_n^{(n-1)i}\, t^i \\
\sum_{i=0}^{n-1} x_{2,i}\, t^i & \sum_{i=0}^{n-1} x_{1,i}\, \omega_n^i\, t^i & \sum_{i=0}^{n-1} x_{0,i}\, \omega_n^{2i}\, t^i & \cdots & \delta\sum_{i=0}^{n-1} x_{3,i}\, \omega_n^{(n-1)i}\, t^i \\
\vdots & \vdots & \vdots & \vdots & \vdots \\
\sum_{i=0}^{n-1} x_{n-2,i}\, t^i & \sum_{i=0}^{n-1} x_{n-3,i}\, \omega_n^i\, t^i & \sum_{i=0}^{n-1} x_{n-4,i}\, \omega_n^{2i}\, t^i & \cdots & \delta\sum_{i=0}^{n-1} x_{n-1,i}\, \omega_n^{(n-1)i} t^i \\
\sum_{i=0}^{n-1} x_{n-1,i}\, t^i & \sum_{i=0}^{n-1} x_{n-2,i}\, \omega_n^i\, t^i & \sum_{i=0}^{n-1} x_{n-3,i}\, \omega_n^{2i}\, t^i & \cdots & \sum_{i=0}^{n-1} x_{0,i}\, \omega_n^{(n-1)i}\, t^i
\end{bmatrix}. \qquad (12.a)$$

978-1-4244-2324-8/08/$25.00 © 2008 IEEE.

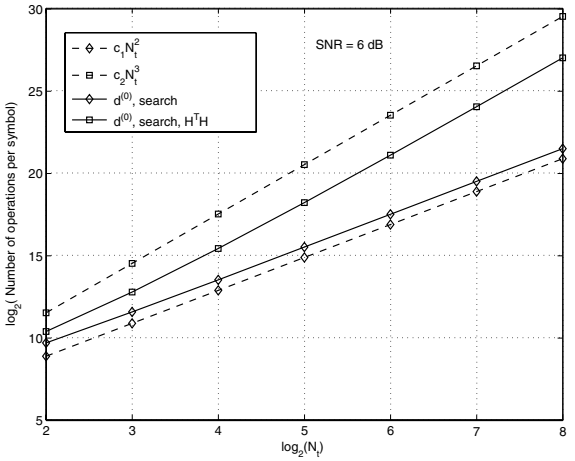

Fig. 1. Computation complexity of the LAS algorithm in decoding non-orthogonal STBCs from CDA. MMSE initial vector. 4-QAM.

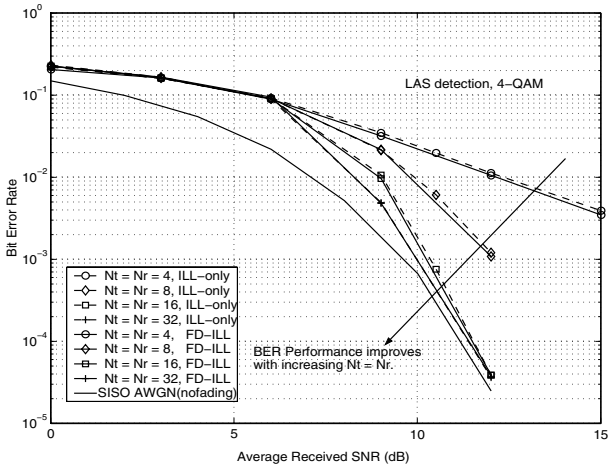

Fig. 2. Uncoded BER performance of the LAS detector for **ILL-only** and **FD-ILL** STBCs for different $N_t = N_r$. 4-QAM, $2N_t$ bps/Hz. *BER improves as $N_t = N_r$ increases. ILL-only STBCs perform as good as FD-ILL STBCs.*

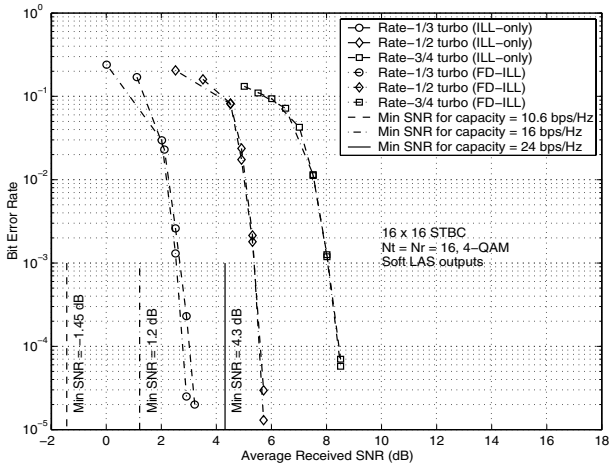

Fig. 3. Turbo coded BER of the LAS detector for 16×16 **ILL-only** and **FD-ILL** STBCs. 4-QAM, turbo code rates: 1/3, 1/2, 3/4 **(10.6, 16, 24 bps/Hz)**. *LAS detector performs close to within about 4 dB from capacity. ILL-only STBCs perform as good as FD-ILL STBCs.*

IV. Simulation Results and Discussions

In this section, we present the uncoded/turbo coded BER performance of the LAS detector in decoding non-orthogonal STBCs from CDA. We consider two STBC designs, namely, i) 'FD-ILL' STBCs where $\delta = e^{\sqrt{5}\mathrm{j}}$, $t = e^{\mathrm{j}}$ in (12.a), and ii) 'ILL-only' STBCs where $\delta = t = 1$. The SNRs in all the BER performance figures are the average received SNR per received antenna, γ, defined in Sec. II [3]. In all the simulations, we have taken MMSE filter as the initial filter.

Uncoded BER as a function of increasing $N_t = N_r$: In Fig. 2, we plot the uncoded BER performance of the LAS detector in decoding ILL-only and FD-ILL STBCs for $N_t = N_r = 4, 8, 16, 32$ and 4-QAM. SISO AWGN performance (without fading) is also plotted for comparison. It is interesting to observe that the BER improves and gets closer to SISO AWGN performance for increasing $N_t = N_r$. For example, with $N_t = N_r = 16, 32$, for BERs better than 10^{-3}, the performance achieved by the LAS detector is very close to the SISO AWGN performance. This implies that the detector is able to effectively make each of the 1024 data symbols in a 32×32 STBC matrix see almost an independent AWGN-only channel without interference from other symbols (although the symbols are entangled in the STBC matrix to start with). We note that, to our knowledge, this is the first time decoding and near-SISO AWGN BER performance for a 32×32 non-orthogonal STBC from CDA are reported.

Performance of ILL-only versus FD-ILL STBCs: Another observation that can be made in Fig. 2 is that the performance of ILL-only STBCs with LAS detection for $N_t = N_r = 4, 8, 16$ and 4-QAM are as good as those of the corresponding FD-ILL STBCs. A similar closeness between the performance of ILL-only and FD-ILL STBCs is observed in the turbo coded BER performance as well, which is shown in Fig. 3 for a 16×16 STBC with 4-QAM and turbo code rates of 1/3, 1/2 and 3/4. This is an interesting observation, since this suggests that, in such cases, the computational simplicity with $\delta = t = 1$ in ILL-only STBCs can be taken advantage of without incurring much performance loss compared to FD-ILL STBCs for which $\delta = e^{\sqrt{5}\mathrm{j}}$, $t = e^{\mathrm{j}}$.

Turbo coded BER and nearness-to-capacity results: In all the turbo coded BER simulations, we fed the soft LAS outputs presented in Sec. III-A as input to the turbo decoder. In Fig. 3, we plot the turbo coded BER of the LAS detector in decoding 16×16 FD-ILL and ILL-only STBCs, with 4-QAM and turbo code rates 1/3 (10.6 bps/Hz), 1/2 (16 bps/Hz), 3/4 (24 bps/Hz). The minimum SNRs required to achieve these capacities $\big($obtained through the ergodic capacity expression in [1]$\big)$ are also shown. It can be observed that the LAS detector performs close to within just about 4 dB from capacity. Also, the coded BER performance of FD-ILL and ILL-only STBCs are almost the same. Figure 4 shows the coded BER and nearness to capacity results of the LAS detector in decoding 32×32 ILL-only STBC with 16-QAM and turbo code rates 1/3 (42.6 bps/Hz), 1/2 (64 bps/Hz), 3/4 (96 bps/Hz), where performance close to within about 10 dB from capacity are observed to be achieved.

Performance in asymmetric MIMO with $N_r < N_t$: In the performance plots in Figs. 2 to 4, we have considered $N_t = N_r$. Asymmetric MIMO scenarios where $N_r < N_t$ are of practical interest; while large N_t can be provided at the base stations, a smaller N_r may be preferred at the user terminals. In this context, we evaluated the performance of the LAS detector for $N_r < N_t$ for 8×8 and 16×16 ILL-only STBCs.

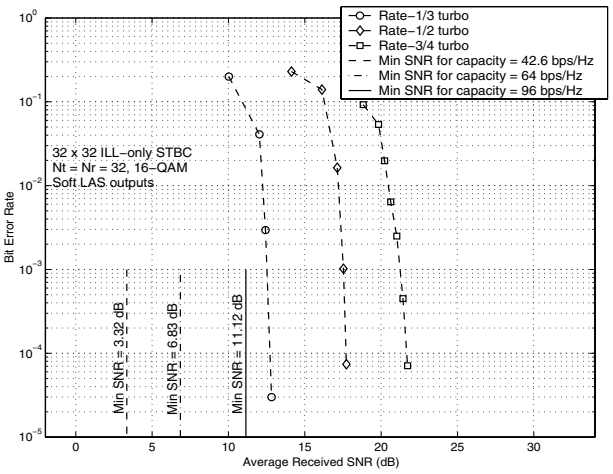

Fig. 4. Turbo coded BER of the LAS detector for **32** x **32 ILL-only** STBC. **16-QAM**, turbo code rates: 1/3, 1/2, 3/4 **(42.6, 64, 96 bps/Hz)**. *The LAS detector performs close to within about 10 dB from capacity*.

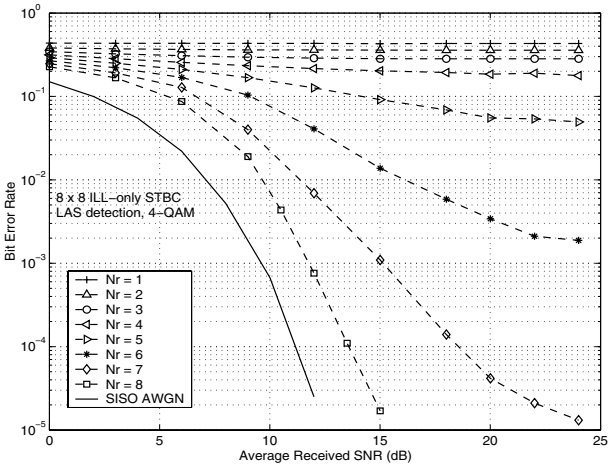

Fig. 5. Uncoded BER of the LAS detector in asymmetric MIMO with $N_r < N_t$. 8×8 ILL-only STBC, $N_t = 8$, 4-QAM. *Good BER performance is achieved even with* $N_r = 6, 7$

Figure 5 shows the uncoded BER performance of the LAS detector for 8×8 ILL-only STBC with $N_t = 8$ and 4-QAM for different values of $N_r \leq 8$. It can be observed that decreasing N_r results in degraded BER compared to that for $N_r = 8$, causing error floors. This is expected as the receive signal dimension is less than that of the transmit signal dimension for $N_r < N_t$. However, the BER degradation is not catastrophic when $N_t - N_r$ is small. Particularly, the error floors occur at sufficiently low BERs $\big($e.g., $< 2 \times 10^{-3}$ for up to $N_r = 6\big)$. Such low uncoded BERs are sufficiently small for the outer turbo codes to be effective. We illustrate this point in Fig. 6, where we show the coded BER plots of LAS detector in decoding 16×16 ILL-only STBC with $N_t = 16$, $N_r = 12$, 4-QAM, and turbo code-rates of $1/3, 1/2, 3/4$. It can be seen that the LAS detector is able to achieve close to within about 8 dB from theoretical capacity, indicating its effectiveness even in asymmetric MIMO systems with $N_r < N_t$.

V. Conclusions

We presented a near-ML low-complexity algorithm for the detection of large, high-rate, non-orthogonal STBCs from CDA with tens of antennas. We note that we have decoded perfect codes of large sizes also using the LAS detector. With the feasibility of such low-complexity detectors, large MIMO systems with tens of antennas and high spectral efficiencies can become practical, enabling interesting high data rate wireless applications (e.g., wireless IPTV distribution). The low-complexity feature of the LAS detector can allow the inclusion of 4×4, 8×8, 16×16 non-orthogonal STBCs from CDA into wireless standards like IEEE 802.11n and IEEE 802.16e, which can allow higher spectral efficiencies than those that are currently possible in these standards.

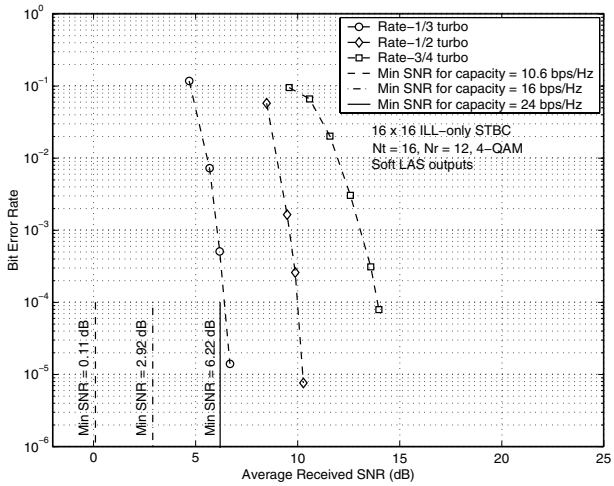

Fig. 6. Turbo coded BER of the LAS detector in asymmetric MIMO with $N_r < N_t$. 16×16 ILL-only STBC, $N_t = 16$, $N_r = 12$, 4-QAM, turbo code rates: 1/3, 1/2, 3/4 (10.6, 16, 24 bps/Hz). *The LAS detector performs close to within about 8 dB from capacity.*

References

[1] I. E. Telatar, "Capacity of multi-antenna Gaussian channels," *European Trans. Telecommun.,* vol. 10, no. 6, pp. 585-595, November 1999.

[2] A. Paulraj, R. Nabar, and D. Gore, *Introduction to Space-Time Wireless Communications*, Cambridge University Press, 2003.

[3] H. Jafarkhani, *Space-Time Coding: Theory and Practice*, Cambridge University Press, 2005.

[4] S. M. Alamouti, "A simple transmit diversity technique for wireless communications," *IEEE JSAC*, vol. 16, pp. 1451–1458, October 1998.

[5] V. Tarokh, H. Jafarkhani, and A. R. Calderbank, "Space-time block codes from orthogonal designs," *IEEE Trans. Inf. Theory,* vol. 45, no. 5, pp. 1456-1467, July 1999.

[6] B. A. Sethuraman, B. S. Rajan, and V. Shashidhar, "Full-diversity high-rate space-time block codes from division algebras," *IEEE Trans. Inf. Theory*, vol. 49, no. 10, pp. 2596-2616, October 2003.

[7] E. Viterbo and J. Boutros, "A universal lattice code decoder for fading channels," *IEEE Trans. Inf. Theory,* pp. 1639-1242, July 1999.

[8] M. O. Damen, H. El Gamal, G. Caire, "On maximum-likelihood detection and the search for the closest lattice point," *IEEE Trans. Inf. Theory*, pp. 2389-2401, October 2003.

[9] B. Hassibi, H. Vikalo, "On the sphere-decoding algorithm I. Expected complexity," *IEEE Trans. Sig. Proc.,* pp. 2806-2818, August 2005.

[10] X. Yang, Y. Xiong, F. Wang, "An adaptive MIMO system based on unified belief propagation detection," *Proc. IEEE ICC'2007*, June 2007.

[11] B. Farhang-Boroujeny, H. Zhu, and Z. Shi, "Markov chain Monte Carlo algorithms for CDMA and MIMO communication systems," *IEEE Trans. on Sig. Proc.,* pp. 1896-1908, May 2006.

[12] Y. Sun, "A family of linear complexity likelihood ascent search detectors for CDMA multiuser detection," *Proc. IEEE Intl. Symp. on Spread Spectrum Tech. & App.,* September 2000.

[13] K. Vishnu Vardhan, S. K. Mohammed, A. Chockalingam, B. Sundar Rajan, "A low-complexity detector for large MIMO systems and multi-carrier CDMA systems," *IEEE JSAC*, vol. 26, pp. 473-485, April 2008.

[14] S. K. Mohammed, K. Vishnu Vardhan, A. Chockalingam, and B. Sundar Rajan, "Large MIMO Systems: A low-complexity detector at high spectral efficiencies," *Proc. IEEE ICC'2008*, May 2008.

[15] Saif K. Mohammed, A. Chockalingam, and B. Sundar Rajan, "A low-complexity near-ML performance achieving algorithm for large MIMO detection," *Proc. IEEE ISIT'2008*, July 2008.

[16] B. Hassibi and B. Hochwald, "High rate codes that are linear in space and time," *IEEE Trans. Inf. Theory*, pp. 1804-1824, July 2002.